

Fluorescence EEMs and PARAFAC Techniques in the Analysis of Petroleum Components in the Water Column

Zhengzhen Zhou, Laodong Guo, and Christopher L. Osburn

Abstract

Fluorescence excitation–emission matrix (EEM) techniques coupled with parallel factor (PARAFAC) modeling have been used in the diagnosis and identification of petroleum and hydrocarbon components in aquatic environments. Here, we provide detailed protocols for the use of UV–Vis spectroscopy and fluorescence spectroscopy and for data acquisition and processing. UV absorbance at different wavelengths is used to derive optical properties, such as absorption coefficient at 254 nm (a_{254}), specific UV absorbance ($SUVA_{254}$), and spectral slopes at different wavelength intervals (e.g., $S_{275-295}$) or slope ratio, and data of fluorescence EEMs are used to identify major fluorescence components. In addition, $SUVA_{254}$ and spectral slope values are related to aromaticity and molecular weights of dissolved organic matter (DOM). Oil-related fluorescent components and specific polycyclic aromatic hydrocarbon (PAH) compounds could be readily identified using fluorescence EEMs, especially when combined with PARAFAC analysis. During and after the Deepwater Horizon oil spill in the Gulf of Mexico, three oil components were found in the water column with maximum Ex/Em at 224–226/328–340, 232–244/346–366, and 264–252/311–324 nm, respectively. Major PAH compounds identified include naphthalene, fluorene, phenanthrene, and others. Oil component ratios can also serve as an indicator for oil degradation status. Optical properties especially fluorescence signatures and fluorescence component ratios serve as a complement to other chemical and molecular analyses of petroleum and hydrocarbon components in seawater.

Keywords: Fluorescence EEMs, Hydrocarbon, Oil components, PARAFAC analysis, UV absorbance

1 Introduction

Petroleum contains diverse hydrocarbons and other organic compounds such as polycyclic aromatic hydrocarbon (PAH) compounds that have delocalized electrons within the aromatic rings and that are optically active and can absorb ultraviolet–visible (UV–Vis) light and fluoresce [1]. Thus, the presence of optically active compounds, either extracted or dispensed in seawater, could be readily determined and characterized by UV–Vis spectroscopy and fluorescence spectroscopy techniques [2–8]. Similarly, dissolved organic matter (DOM) in aquatic environments with different composition and sources can also be effectively characterized by

its optical properties, such as UV–Vis absorbance and fluorescence excitation–emission matrix (EEM) spectra [9–17], especially when parallel factor (PARAFAC) analysis is coupled with fluorescence EEM techniques [18–22]. Indeed, UV–Vis absorption, fluorescence EEM, and PARAFAC techniques have been widely used to characterize, fingerprint, and monitor oil in aquatic systems (e.g., [4, 5, 23–29]), with focus on PAHs due to the detection limit of the optical methodology. Recently, the Deepwater Horizon (DWH) oil spill in the northern Gulf of Mexico had spurred extensive studies on the fate, transport, and transformation of oil components using the optical properties in coastal and oceanic environments [30–35].


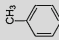
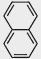
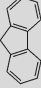
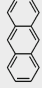
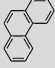
A number of optical parameters derived from UV–Vis absorbance spectra and fluorescence EEMs can provide useful information for the identification and detection of petroleum and hydrocarbon components and their interactions with marine DOM, linking to the abundance, general molecular weight, optical activity, composition, and degradation status (e.g., [34]). From UV–Vis absorbance spectra, parameters such as absorption coefficient (e.g., a_{254}), specific UV absorbance (SUVA, e.g., $SUVA_{254}$), and spectral slope (e.g., $S_{275-295}$) can be acquired. Among these optical properties, a_{254} could be a proxy for dissolved organic carbon (DOC) and an indicator of its abundance, while $SUVA_{254}$ is positively linked to optical reactivity or aromaticity, and the $S_{275-295}$ value is inversely linked to bulk DOM molecular weight [14, 17]. During the DWH oil spill, higher $SUVA_{254}$ and lower $S_{275-295}$ were found in deep waters than in surface waters [34]. These results suggested the presence of aromatic DOM with higher molecular weight and optical activity than most natural DOM in deep waters where the oil leak occurred, reflecting newly introduced crude oil components. Low molecular weight oil components released from the DWH spill were likely subject to preferential degradation and volatilization in the surface waters [36]. Increased spectral slope was also observed in oil degradation experiments, indicating preferential decomposition of aromatic DOM in seawater [35]. Additionally, the relationships among salinity, DOC concentration, a_{254} , and $SUVA_{254}$ in the water column suggested the presence of oil [34]. For example, 3 months after the DWH oil spill was capped, marine DOM characteristics and positive DOC and $SUVA_{254}$ correlation were observed in surface waters of the Gulf of Mexico, whereas high DOM optical yield and negative correlations between DOC and $SUVA_{254}$ were found in deep waters, suggesting sustained influence from oil in deepwater DOM [30, 33].

Based on fluorescence EEM data, fluorescence signatures from petroleum and oil components could be compared with those of PAH standards and linked to specific PAH compounds. Previous studies have examined the specific excitation–emission wavelengths

of many PAH standards (Table 1 and references therein). Although the solvents used in these studies varied from dichloromethane [1], hexane, or chloroform [23] to freshwater [37] and seawater [32], it seems that the peak Ex/Em positions of the PAH standards change little for naphthalene and phenanthrene, but are significantly different among solvents especially for chrysene and perylene (Table 1). Solvent interactions with petroleum and oil components, such as quenching and energy-transfer processes, produce these differences in fluorescence signatures. Oil extracted into nonpolar solvents will thus produce signatures different from oil dissolved into seawater [30]. Thus, when using fluorescence EEM to examine oil, solvent effect should be taken into account.

When combined with PARAFAC analysis, EEMs can be resolved into their underlying fluorescent components [20]. Several typical natural fluorescent DOM components, including humic- and protein-like DOM, have previously been identified (Table 2 and references therein). Using this technique on samples collected from the northern Gulf of Mexico during the DWH oil spill, three oil-related components were identified even after 2 years of the spill (Table 2, Fig. 1). The most dominant oil component, O1, had its maximum Ex/Em at 224–226/328–340 nm, strongly resembling fluorescence signatures to benzene and other PAHs described in Beltrán et al. [37] and Christensen et al. [1]. A second oil component, O2, was likely an oil degradation product from both microbial and photochemical degradation, showing its maximum Ex/Em at 230–250/340–380 nm, exhibiting similar fluorescence fingerprinting and degradation rate as phenanthrene [1, 23, 35]. The third oil component, O3, with Ex/Em ~224, 250–280/310–345 nm, was hypothesized as degradation product mostly from photochemical degradation and showed similar peak Ex/Em positions of naphthalene and fluorene [1, 4, 34, 37]. Additionally, fitting the PAH fluorescence EEMs to the abovementioned components showed that the EEMs of some PAHs can be well explained (100% for naphthalene and fluorene) by their corresponding oil-related components (Table 3). The fluorescence component ratios, such as O2/O1 and O3/O1, are intensive properties that show distinct values between crude oil and weathered oil, as well as between oil and seawater samples. Increasing trend of O2/O1 and O3/O1 was observed in time series field samples taken during and after the DWH oil spill and in laboratory oil degradation experiments [34, 35]. Thus, the fluorescence component ratios likely reflect the degradation status of oil and can be used as indices to track the fate and transformation of oil in aquatic environments, as suggested in Zhou and Guo [33] and Zhou et al. [34].

Table 1
Excitation–emission (Ex/Em) wavelengths of selected polycyclic aromatic hydrocarbon (PAH) compounds

PAH compound	Molecular formula	Structural formula	Mendoza et al. [32]		Christensen et al. [1]		Beitran and Guiteras [37]		Alostaz et al. [23]		Zhou and Guo (unpublished)	
			Solvent: seawater (S = 36.21)	Ex/Em (nm)	Solvent: dichloromethane	Ex/Em (nm)	Solvent: water with surfactant Brij-35	Ex/Em (nm)	Solvent: hexane or chloroform	Em (nm)	Solvent: ultrapure water or seawater	Ex/Em (nm)
Benzene	C ₆ H ₆		225, 250/335, 275, 550	–	–	–	–	–	–	–	–	–
Toluene	C ₇ H ₈		225, 260/280, 415, 560	–	–	–	–	–	285	–	–	–
Naphthalene	C ₁₀ H ₈		225, 230, 275/330, 495	275/330, 345	275/330, 345	225/330, 345	340	275/330, 345	–	–	–	275/330, 345
Fluorene	C ₁₃ H ₁₀		–	260/310, 320	260/310, 320	260/310, 320	–	–	–	–	–	260/305
Anthracene	C ₁₄ H ₁₀		250/380, 400, 420	–	–	250/380, 405, 425	–	–	–	–	–	250/380, 400, 420
Phenanthrene	C ₁₄ H ₁₀		250, 290/345, 360	250/350, 370	250/350, 370	255/350, 370	360	255/350, 370	360	–	–	255/350, 370

(continued)

Table 1
(continued)


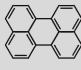
PAH compound	Molecular formula	Structural formula	Mendoza et al. [32]	Christensen et al. [1]	Beltran and Guiteras [37]	Alostaz et al. [23]	Zhou and Guo (unpublished)
			Solvent: seawater (S = 36.21) Ex/Em (nm)	Solvent: dichloromethane Ex/Em (nm)	Solvent: water with surfactant Brij-35 Ex/Em (nm)	Solvent: hexane or chloroform Em (nm)	Solvent: ultrapure water or seawater Ex/Em (nm)
Pyrene	C ₁₆ H ₁₀		–	–	245, 275/320, 400	400, 420, 480	240/380
Perylene	C ₂₀ H ₁₂		225, 235, 330/335, 380, 560	255, 390/445, 470	255/445, 475	–	240/380

Table 2
Fluorescent DOM components identified and reported in previous studies [33–35, 38–40]

Label	Excitation wavelength (nm)	Emission wavelength (nm)	Type of fluorophores
A	260	380–460	UV humic-like
C	320–360	420–460	Visible terrestrial humic-like
M	290–310	370–410	Visible marine humic-like
B	230, 275	305	Tyrosine-like, protein-like
T	230, 275	340	Tryptophan-like, protein-like
O1	224–226	328–340	Dominant oil component from MC252 crude oil
O2	232–244	346–366	Degradation product from both microbial and photochemical degradation
O3	264–252	311–324	Degradation product mostly from photochemical degradation

Optical analysis, especially using the fluorescence spectroscopy, is able to detect oil in the water column with high sensitivity, but limited to measurements of optically active oil components, such as PAHs. In this chapter, we describe the use of UV–Vis and fluorescence spectroscopy techniques to obtain optical parameters and to identify oil components and selected PAH compounds in water samples for elucidating abundance, composition, degradation status of petroleum, and hydrocarbon components in aquatic environments.

2 Materials

2.1 Materials for Measurements of UV–Vis Absorbance

Instrument: UV–Vis spectrophotometer (e.g., Cary 300 Bio; Agilent 8453, Agilent Technologies, USA)

Cuvette: 10-cm path-length quartz cuvette (e.g., Starna Cells, Inc., USA, www.starnacells.com)

2.2 Materials for Measurements of Fluorescence EEMs

Instrument: Spectrofluorometer (e.g., Shimadzu RF-5301PC, Shimadzu Corp., Kyoto, Japan; Horiba Fluoromax-4, Horiba Jobin Yvon, Inc., Japan)

Software for collecting EEMs, e.g., Panorama fluorescence 1.1 software (LabCognition, Dortmund, Germany) and FluoEssence V3.5 (Horiba, Japan)

Cuvette: 4.5 mL UV-grade quartz cuvette (10 mm light path) (e.g., Starna Cells, Inc., USA, www.starnacells.com)

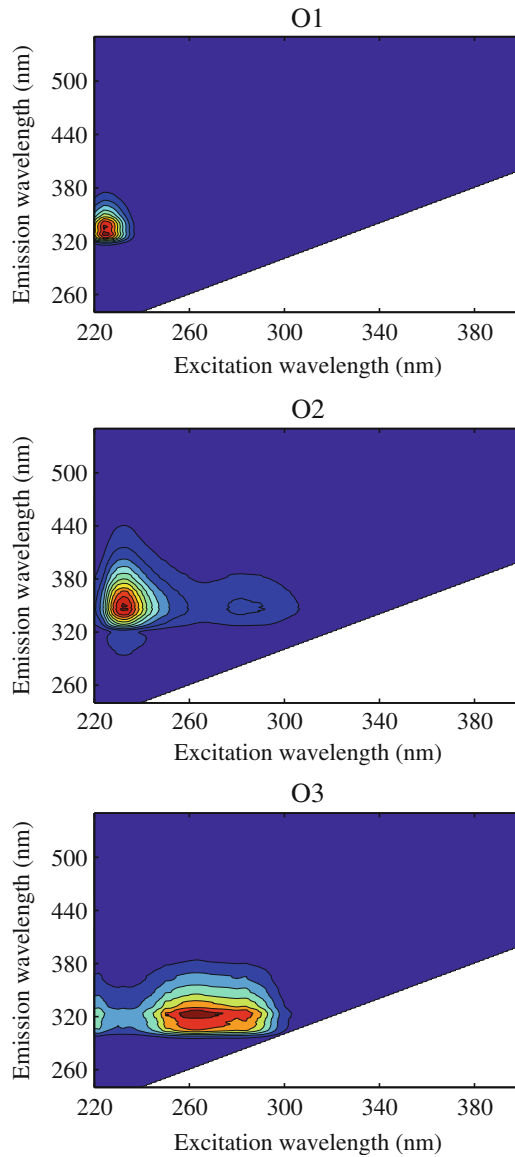


Fig. 1 Oil-related components identified from water samples collected in the northern Gulf of Mexico during and after the Deepwater Horizon oil spill based on coupling fluorescence excitation–emission matrix (EEM)-PARAFAC techniques

2.3 Materials for Cleaning Cuvette

Hexane (e.g., Sigma, <http://www.sigmaaldrich.com>)

Methanol (e.g., Sigma, <http://www.sigmaaldrich.com>)

Acetone (e.g., Sigma, <http://www.sigmaaldrich.com>)

Dichloromethane (e.g., Sigma, <http://www.sigmaaldrich.com>)

Table 3
Selected PAH compounds in the oil-related components identified from oil-impacted seawater samples collected from the northern Gulf of Mexico

	Corresponding oil-related component	Percentage explained by this component
Phenanthrene	O2	82
Pyrene	O2	79
Anthracene	O2	69
Naphthalene	O3	100
Fluorene	O3	100

2.4 Materials for the Calibration of Fluorescence Intensity

Quinine sulfate dihydrate (e.g., Sigma, <http://www.sigmaaldrich.com>), stored in dark at $\sim 4^{\circ}\text{C}$.

3 Methods

This protocol describes the use of a UV–Vis spectrophotometer and a fluorescence spectrophotometer to collect UV–Vis absorbance and fluorescence EEMs of natural water samples, as well as how to correct spectra and how to apply PARAFAC analysis to fluorescence EEMs to identify petroleum and DOM components (Fig. 2).

3.1 UV–Vis Absorption Spectra

3.1.1 Collection of UV–Vis Absorbance

1. Allow samples (*see Note 1*) to warm up to room temperature in a constant-temperature laboratory (e.g., 20°C).
2. Transfer the sample into the cuvette after the cuvette has been cleaned with organic solvents to make sure cuvette is free from cross-contamination of oil and has been rinsed with the water sample for three times (*see Note 2*).
3. Collect UV–Vis absorption spectra over decided wavelength ranges (e.g., 200–1,100 nm) with appropriate increments (e.g., 1 nm).
4. In order to minimize the inner-filter effect, if a sample has absorbance higher than 0.02 at 260 nm, dilute the sample with ultrapure water to decrease its absorbance to lower than 0.02 [41].
5. Collect a scan of ultrapure water ($18.2\text{ M}\Omega$) each analytical day in the same manner for the samples to blank correct the spectra.

3.1.2 UV–Vis Absorbance Data Processing

1. Subtract the absorbance of water blank.
2. Subtract the average absorbance between 650 and 800 nm to correct for the refractive index effect [42].

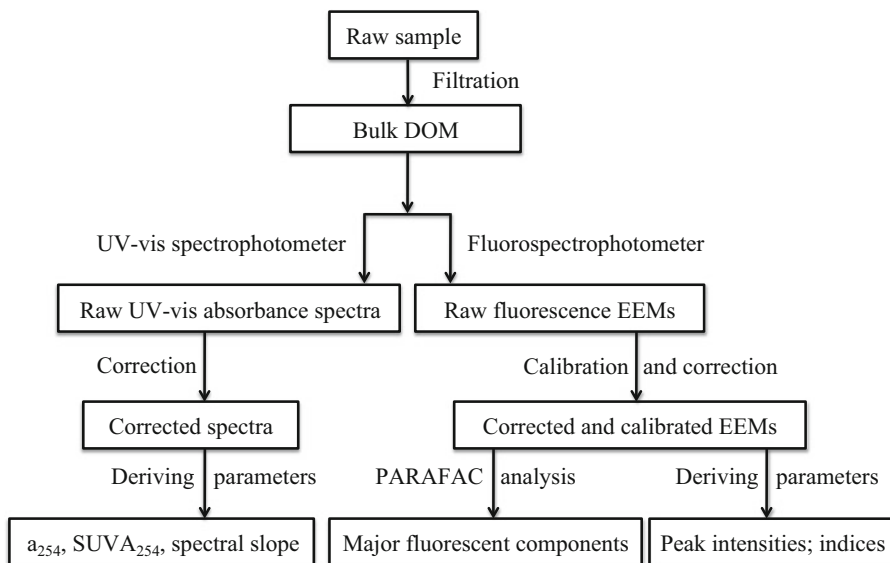


Fig. 2 Flowchart showing acquisition of UV-Vis spectra and fluorescence EEM and derivation of fluorescent components and parameters, such as absorption coefficient (a_{254}), specific UV absorbance ($SUVA_{254}$), spectral slope, and fluorescence indices

- Convert absorbance at specific wavelengths (e.g., 254, 355, 412 nm) into Napierian absorption coefficients (a_{254} , a_{355} , a_{412}) based on the following equation:

$$a_{(\lambda)} = A_{(\lambda)} * 2.303/l$$

where $a_{(\lambda)}$ is the absorption coefficient (in m^{-1}) at a specific wavelength (λ), $A_{(\lambda)}$ is the absorbance at wavelength λ , and l is the light path length in meters (Fig. 3). While $A_{(\lambda)}$ is dimensionless, $a_{(\lambda)}$ has a dimension in m^{-1} .

- Calculate specific UV absorbance (SUVA) value by dividing the decadal UV absorbance by respective DOC concentration (mg-C/L, Fig. 3), with a dimension of L/mg-C/m.
- Calculate spectral slope (S) via either linear or nonlinear regression over a specific wavelength interval (e.g., 275–295 nm, 290–400 nm, 350–400 nm) using the following equation:

$$a_{(\lambda)} = Ae^{-S\lambda} + O$$

where $a_{(\lambda)}$ is absorption coefficient at wavelength λ , A is the amplitude, S is the spectral slope (in nm^{-1}), and O is the offset [14, 34, 43] (Fig. 3).

UV-Vis Absorption Spectra
of PAH Compounds

- Dissolve PAH compounds with ultrapure water. Final concentration is ~1 to 2 $\mu g/L$ at saturation.

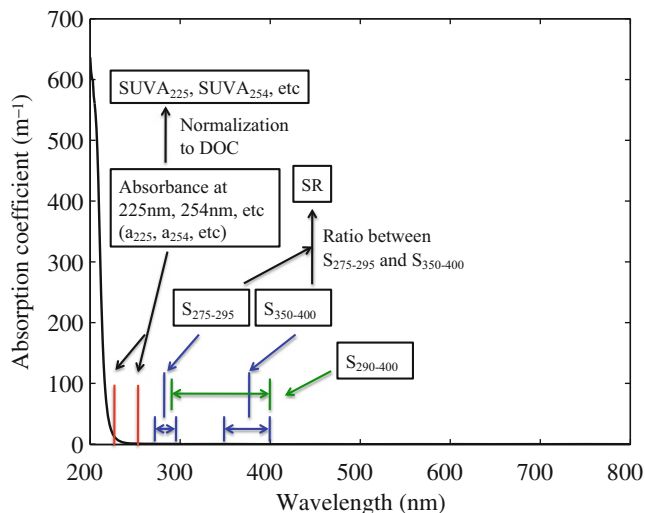


Fig. 3 Examples of UV–Vis absorbance spectrum and schematic of acquiring derived parameters, such as a_{254} , $SUVA_{254}$, and spectral slope (e.g., $S_{275-295}$ and $S_{350-400}$)

2. Acquire UV–Vis absorption spectra of PAH compounds following methods described above. Example spectra of selected PAHs are shown in Fig. 4 (upper and mid panels). Although each PAH has its own characteristic spectra and peaks, none of their peaks were exhibited in the spectra of crude oil-contaminated seawater collected from the Gulf of Mexico right after the DWH oil spill (bottom left panel) [34], even when the sample’s fluorescence signature clearly shows oil characteristics (bottom right panel). UV–Vis absorption spectra of seawater samples collected 6 and 18 months after the spill also did not exhibit PAH peaks. Therefore, the UV–Vis absorbance is not a sensitive parameter for detecting or identifying specific PAH compounds.

3.2 Fluorescence EEMs

3.2.1 Acquisition of Fluorescence EEMs

1. Transfer sample into the cuvette after the cuvette has been cleaned with organic solvents to make sure cuvette is free from cross-contamination of oil and has been rinsed with the specific sample for three times (*see Note 3*).
2. Set predetermined excitation and emission slit widths (e.g., 5 nm for both) and integration time (e.g., 0.5 s).
3. Choose “ratio” mode for the instrument if it is applicable. This will enable light source correction using built-in reference detector. If not applicable, correction needs to be made by hand using concentrated Rhodamine B solution ([20] and reference therein).

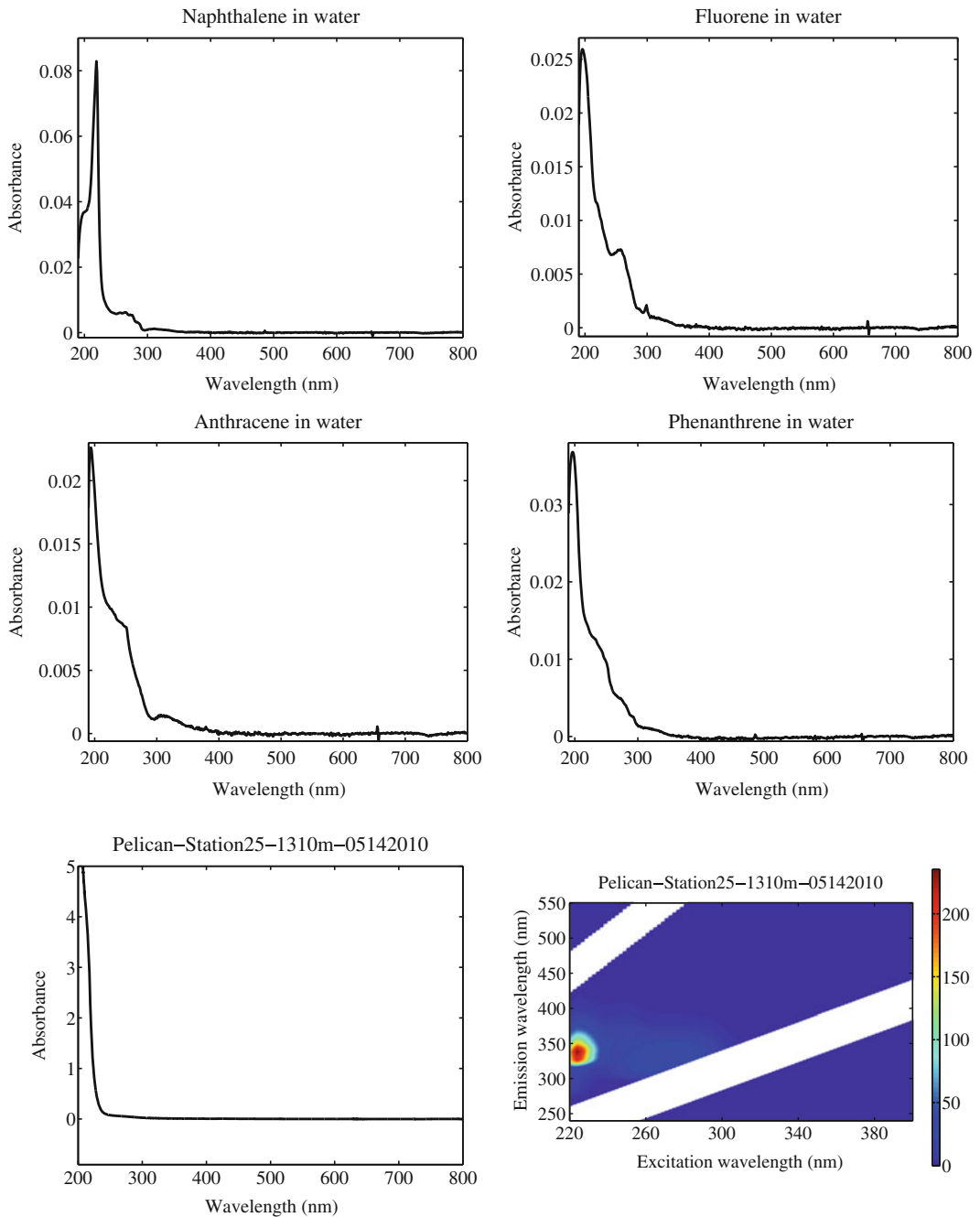


Fig. 4 UV-Vis absorbance spectra of four PAH standards, naphthalene, fluorene, anthracene, and phenanthrene (*upper and mid panels*), and an oil-contaminated seawater sample (*bottom left panel*). No PAH signature peaks were shown in the spectra of the seawater samples, even when the fluorescence EEM of this sample (*bottom right panel*) shows strong oil characteristics

4. Generate fluorescence spectra of samples by recording a series of emission spectra over a wavelength range that covers most naturally occurring fluorescent DOM (e.g., from 240 to 680 nm with 1 nm step) under excitation wavelengths that correspond to natural DOM as well (e.g., from 220 to 400 nm with a 2 nm step).
5. Collect a scan of pure water each analytical day in the same manner as for the samples in order to blank correct the spectra.
6. Measure a series of quinine sulfate standards (e.g., 1, 5, 10, 20, 50 ppb) at Ex/Em 350/450 nm, and perform regression to determine the fluorescence intensity of 1 ppb quinine sulfate.

3.2.2 Fluorescence EEM
Data Processing (see
Note 4)

1. Perform spectral corrections caused by instrumental bias, including light source correction and emission correction, usually supplied with the instrument.
2. Remove the first- and second-order Raman and Rayleigh scattering peaks (see Note 5).
3. Normalize spectral intensity to that of 1 ppb quinine sulfate to yield the unit of ppb quinine sulfate equivalents (QSE).
4. Generate blank corrected data by subtracting the water blank. This completes the correction and calibration of EEMs and makes the EEMs ready for plotting (see Note 6; e.g., Fig. 5) and further analysis.

Identification of Natural
CDOM Components

Table 2 shows the excitation–emission (Ex/Em) wavelength pairs of several natural DOM peaks previously identified. Locate the positions of fluorescence maxima (Ex/Em), and compare them with the fluorescent DOM in the samples.

Fluorescence Signatures
of PAH Compounds

Table 1 provides the fluorescence Ex/Em pairs of selected PAH compounds (see also fluorescence EEMs shown in Fig. 6). Locate the positions of fluorescence maxima (Ex/Em), and compare them with those of PAHs to identify petroleum and oil components present (see Note 7). Note the overlap of Ex/Em maxima for peaks B and T and naphthalene.

Derivation of Indices
(FI, BIX, and HIX)

Calculate indices such as fluorescence index (FI), biological index (BIX), and humification index (HIX) to get information about DOM sources, importance of autochthonous DOM, and the extent of humification (see Fig. 7).

1. The fluorescence index (FI) is the ratio between fluorescence intensities at emission wavelength of 450 and 500 nm at the excitation wavelength of 370 nm.

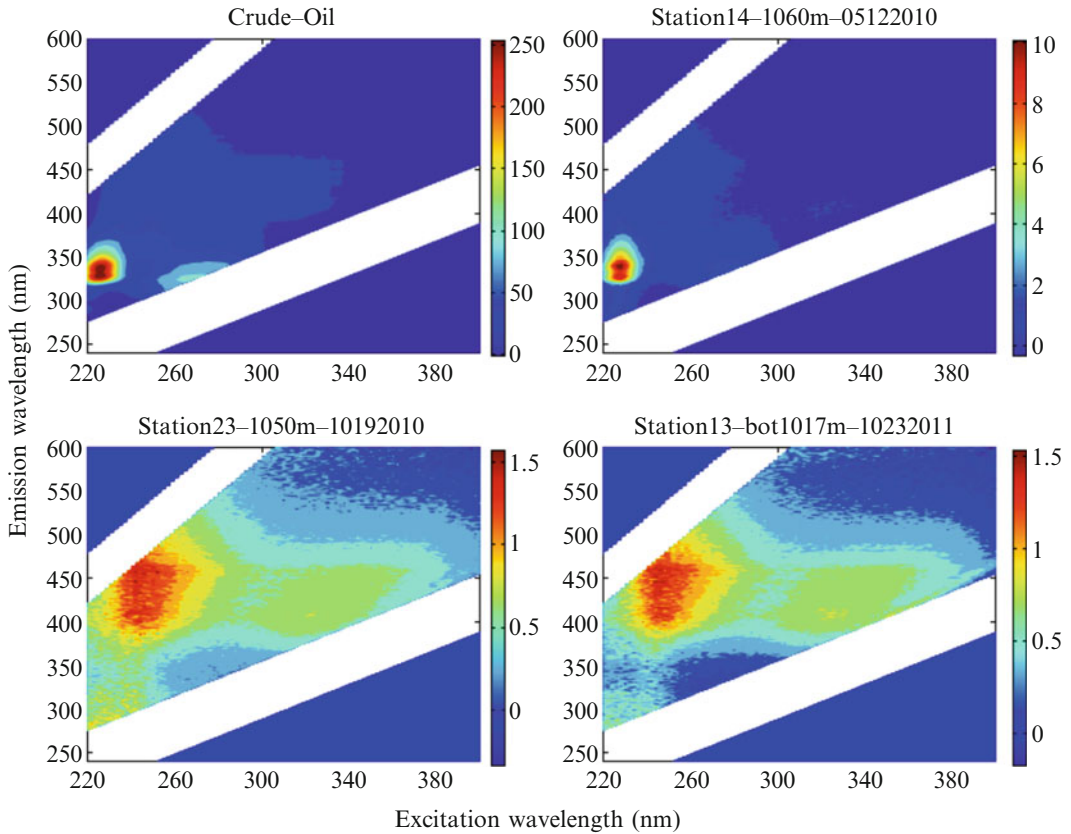


Fig. 5 Examples of fluorescence EEMs of crude oil MC252 (*upper left panel*) and seawater samples taken during DWH oil spill (May 2010, *upper right panel*), 3 months (October 2010, *lower left panel*), and 15 months (October 2011, *lower right panel*) after the spill was capped, respectively

2. The biological index (BIX) is defined as the ratio between fluorescence intensities of 380 and 430 nm at the excitation wavelength of 310 nm.
3. Humification index (HIX) is defined by the ratio of integrated emission of 300–345 nm to integrated emission of 435–480 nm, both measured at an excitation wavelength of 254 nm.

PARAFAC Modeling

PARAFAC modeling is a multi-way fitting analysis technique in which the residual of the sum of squares of the datasets (fluorescence EEMs of all samples) is minimized following the equation:

$$x_{ijk} = \sum_{f=1}^F a_{if} b_{jf} c_{kf} + e_{ijk}$$

where X_{ijk} is fluorescence intensity of the i th sample at the j th emission mode and k th excitation mode and the a_{if} , b_{jf} , and c_{kf} are

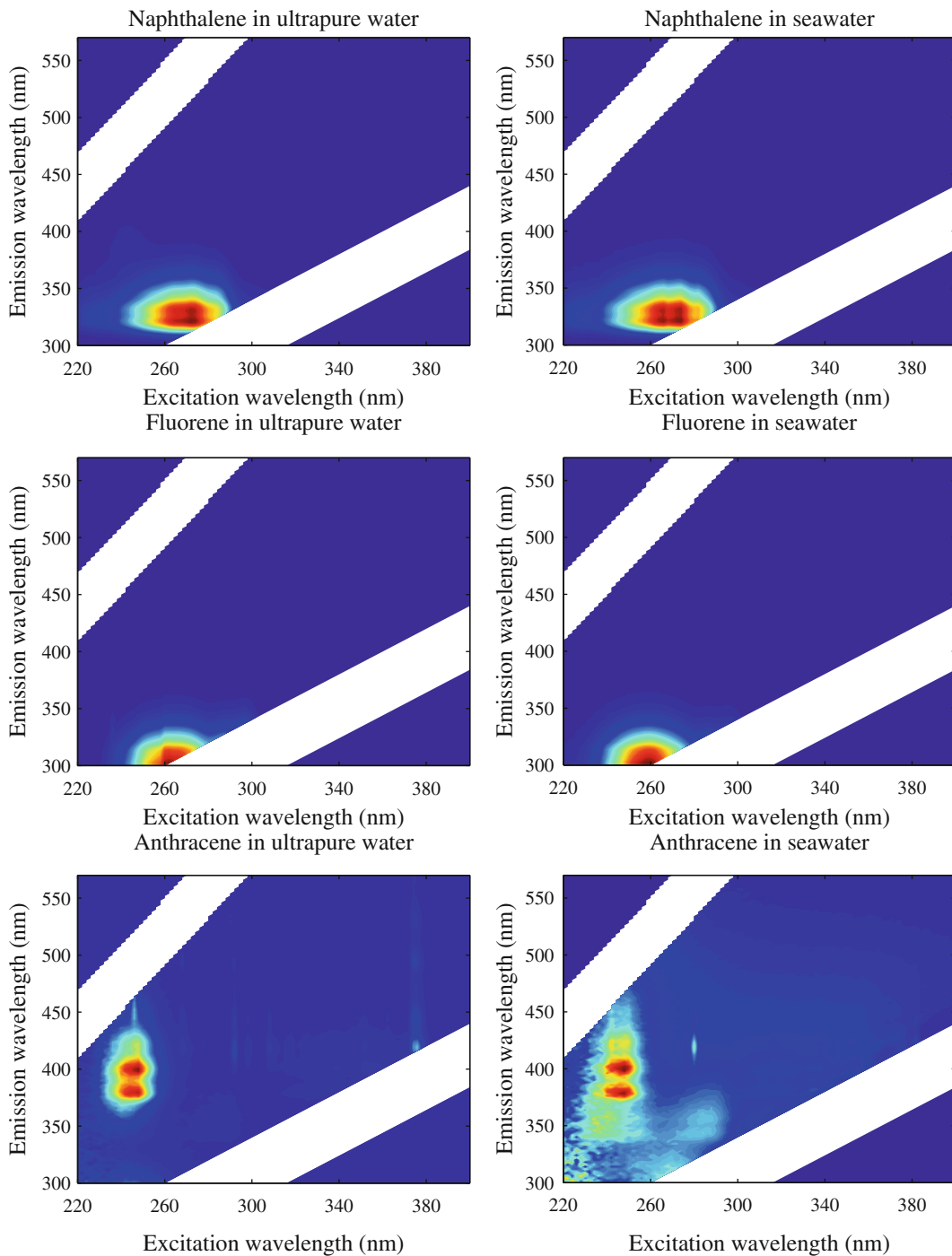


Fig. 6 Fluorescence EEMs of selected PAH compounds in ultrapure water (*left panels*) and seawater (*right panels*)

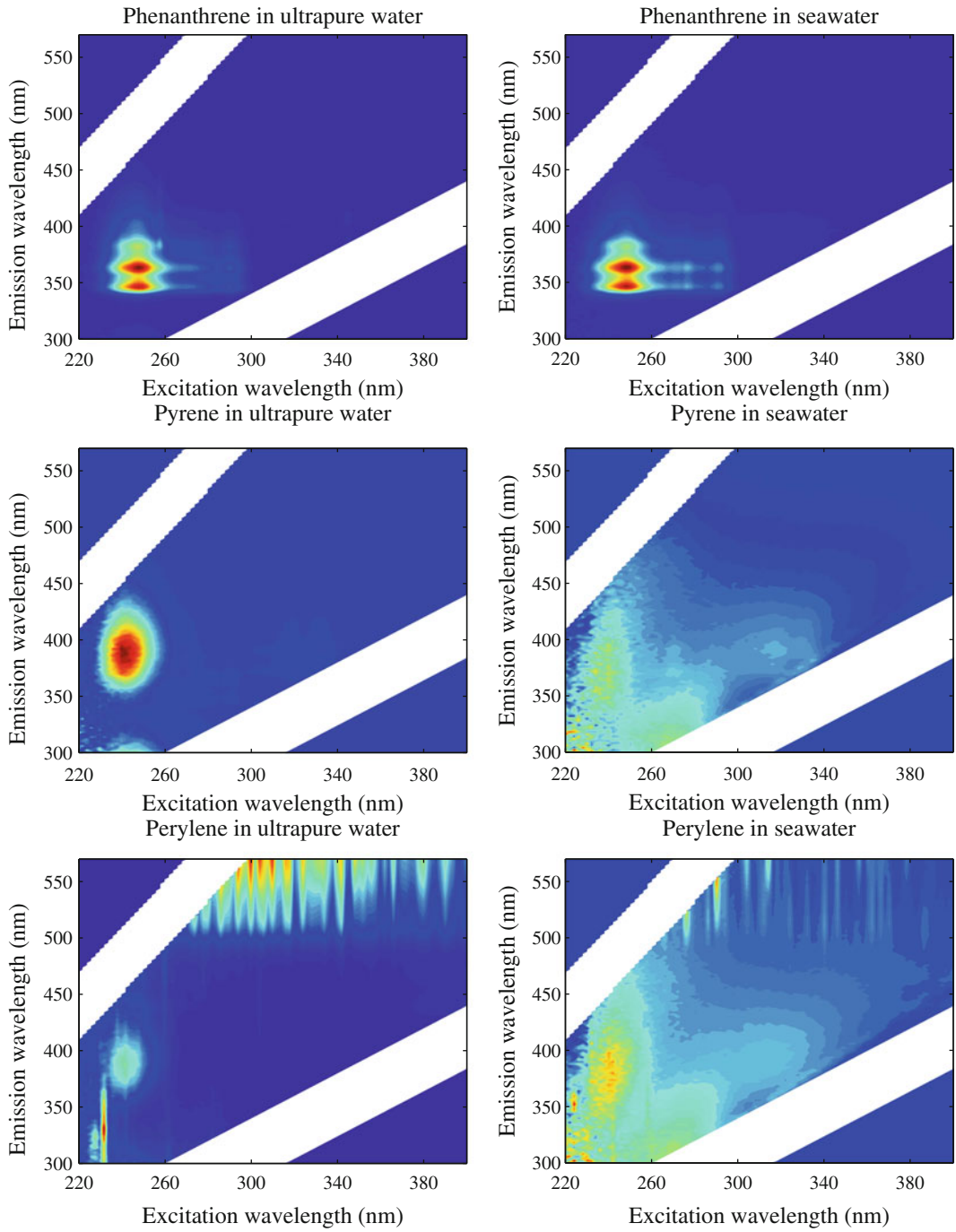


Fig. 6 (continued)

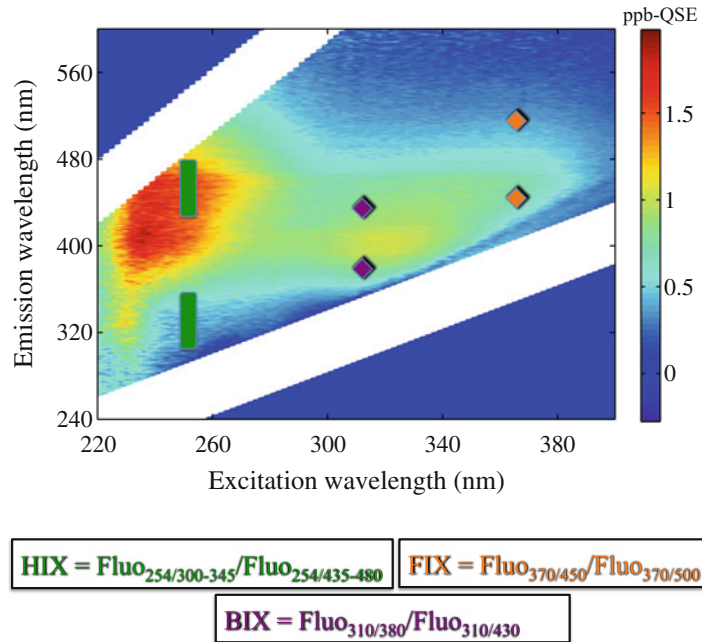


Fig. 7 Schematic showing the acquisition of derived indices including FIX, BIX, and HIX from fluorescence excitation–emission matrices

the scaled parameters that describe the sample and variable for each individual component. The ϵ_{ijk} is the residual not explained by the model.

The application of PARAFAC is based on some assumptions, including adherence to Beer–Lambert law and the absence of interactions between different components. The latter does not hold for natural DOM, so it is important that users understand this caveat [12]. The former is generally true for natural DOM when sample concentration is low and has limited inner-filter effect [44]. Figure 8 exhibits a strong interrelationship between concentrations of fluorene in ultrapure water and the fluorescence intensity at Ex/Em 260/310 nm, showing obedience to the Beer–Lambert law for fluorene at the concentrations between 7.5 and 60 $\mu\text{g L}^{-1}$ (Fig. 8). Other PAH standards are also very sensitive to fluorescence measurement and have shown linear relationship between concentration and fluorescence intensity at peak position [45], obeying the Beer–Lambert law (Table 4). Thus, qualitative and quantitative information about oil components could be derived from PARAFAC analysis of oil-contaminated water column.

Conduct PARAFAC modeling analyses in MATLAB (MathWorks, Fig. 9) using the DOMFluor toolbox ([20]; see Note 8).

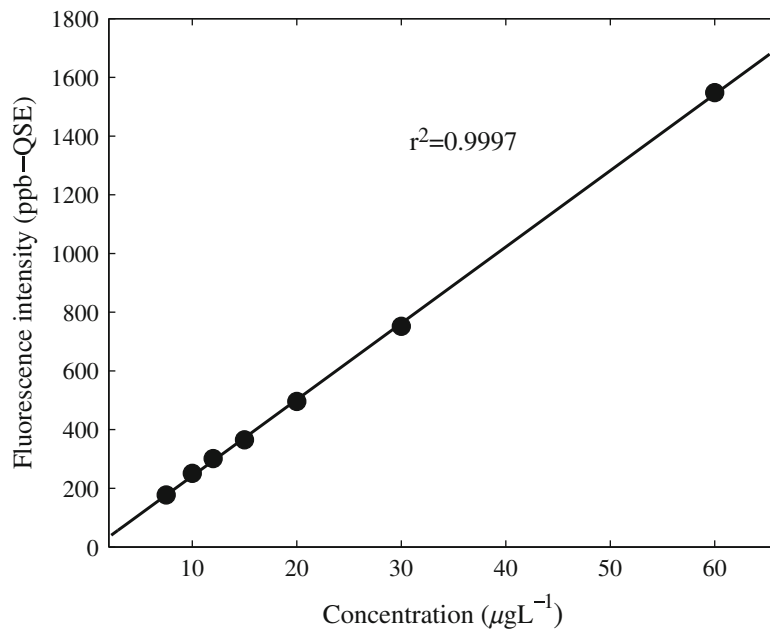


Fig. 8 An example showing the linear relationship between fluorene concentration and fluorescence intensity (ppb QSE) at Ex/Em 260/310 nm

Table 4

The linear relationship between fluorescence intensity at peak position and concentration for selected PAH standards

PAHs	Ex/Em (nm)	Slope (QSE $\text{L}\mu\text{g}^{-1}$)	y-intercept ($\mu\text{g L}^{-1}$)	r^2
Naphthalene	220/334	4.0 ± 0.1	2.4 ± 0.5	0.98
Fluorene	260/310	26.4 ± 0.2	1.5 ± 1.8	1.00
Phenanthrene	250/366	11.5 ± 0.1	1.3 ± 0.6	1.00
Anthracene	245/382	25.2 ± 0.5	-3.5 ± 4.0	1.00
Pyrene	240/374	22.7 ± 0.6	8.7 ± 4.7	1.00

Data from Ferretto et al. [45]

1. Insertion of 0 at the lower and upper triangles to speed up the processing.
2. Find and exclude possible outlier(s) and decide the number of components (*see Note 9*).
3. Model validation using residual analysis, split-half analysis, etc.
4. Model output: Fit sample fluorescence EEMs to the best validated model.

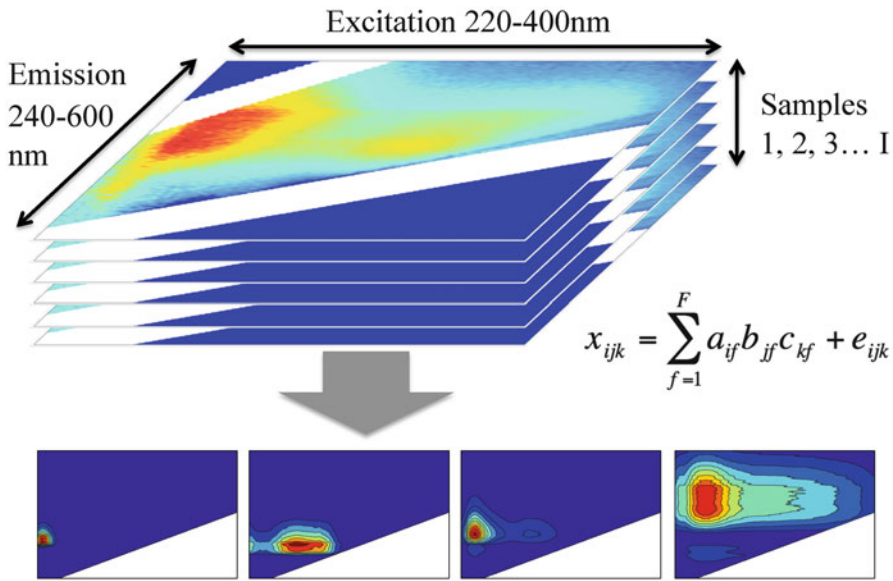


Fig. 9 Schematic showing the application of PARAFAC analysis on fluorescence excitation–emission matrices

Identification of PAH
Compounds in Oil-Related
Fluorescent Components

By fitting the fluorescence EEMs of PAH compounds to the oil components identified from PARAFAC analysis applied to fluorescence EEMs of oil-contaminated seawater samples (e.g., those in [33]), it is shown how much each PAH compound could be explained by the oil-related components (Table 3). For example, up to 100% of the naphthalene and fluorene signals could be explained by O3, which is expected because the fluorescence fingerprint of O3 is so similar to these two PAHs. Similarly, phenanthrene could be largely (up to 81%) explained by O2. Indeed, in a laboratory experiment, among all the PAHs, phenanthrene showed the most similar degradation pathway to O2 [35]. These examples show a close link between PAH compounds and oil-related fluorescent components and further attest the application of fluorescence spectroscopy to the identification of petroleum and oil components. Specifically:

1. Have the model holding fluorescent characteristics (Ex/Em wavelengths) of the oil-related components ready.
2. Fit the fluorescence EEMs of PAH compounds to the model. Presence of these PAHs in the oil-related components is then quantified.
3. Calculate the percentage (similarity) of each PAH compound in each PARAFAC component (*see Note 10*).
4. Identify corresponding fluorescence components with a high percentage (e.g., higher than 75%) for PAHs.

3.3 Statistical Comparisons of PARAFAC Components

3.3.1 Spectral Matching for Similarity Using Tucker's Congruence Coefficient

Tucker's congruence coefficient (TCC) is a mathematical approach to compare similarity between factors from factor analysis methods such as PARAFAC [46]. The mathematics of TCC is beyond the scope of this chapter, but the function is implicit to split-half validation procedures used in the DOMFluor toolbox (e.g., the TCC command; [20]). A critical congruence level of 0.95 is used to determine that two factors can be considered equal. TCC is used to compare the factors (components) of a PARAFAC model during queries to the OpenFluor database (*see* Sect. 3.3.2) but can also be used independently of OpenFluor or DOMFluor. Using the DOMFluor toolbox in MATLAB, execute

```
TCC (Model1, Model2)
A matrix is thus returned :
Model Split half validated
ans =
    0    1    0    0    0    0
    1    0    0    0    0    0
    0    0    1    0    0    0
    0    0    0    1    0    0
    0    0    0    0    1    0
    0    0    0    0    0    1
```

The rows of the matrix indicate components from Model1 and the columns refer to components from Model2. A “1” indicates similarity between the two components such that they are considered identical. A “0” means the components are not identical.

3.3.2 OpenFluor Database

The OpenFluor database (<http://www.openfluor.org>) contains published PARAFAC models and provides a Web-based interface to query one model against many others. New models are submitted, validated, and then added to the database. Querying a model to other PARAFAC models in the literature is done by uploading a text file of excitation and emission spectra for components of the model. In the database, Tucker's congruence coefficient, set at a value of 0.95, is used as the threshold for an identical match between spectra, similar to TCC command in DOMFluor as described above. A table of matches between a queried model and the database is returned to the user. From these results, the user can evaluate the similar of components in a PARAFAC model against many others.

4 Notes

1. Water samples should have already been filtered through a 0.2 μm polycarbonate membrane filters (e.g., Whatman) and stored in pre-combusted (550°C) amber bottles in dark at 4°C before measurements.

- Clean cuvette with acetone, methanol, hexane, and finally dichloromethane to remove any possible residual oil.
- Clean with acetone, methanol, hexane, and finally dichloromethane to effectively take residual oil away from the last sample.
- A statistical software package such as MATLAB or R is recommended for data processing.
- For PARAFAC analysis, not only the scattering peaks, but also the upper and lower triangles should be eliminated for better modeling [20].
- Contour plots are the most widely used type of figure to display an EEM. However, 3D surface plots also are used. These plots can be generated using MATLAB or R.
- Peak positions are subject to change due to the solvent effects, mainly due to the varying polarity of the solvents. With increasing polarity of the solvent, the peak positions of the PAHs would be more redshifted, due to larger energy stabilization caused by solvent relaxation [47, 48]. Thus, attention needs to be given when comparing PAH fluorescence signatures in different solvents.
- Normalizing the EEM of each sample to its own highest (or total) fluorescence intensity (after removal of water scattering peaks) would provide more even loading and more unbiased results [49].
- Constrain the models to nonnegative values to yield chemically reasonable models [20, 50].
- For example, the assigned quantities of phenanthrene in oil components O1, O2, and O3 are 0, 61, and 13 $\mu\text{g/L}$, respectively. The percentage of phenanthrene in O2 would be $61 / (0 + 61 + 13) = 82\%$, which suggests that component O2 is very likely rich in phenanthrene.

References

- Christensen JH, Hansen AB, Mortensen J, Andersen O (2005) Characterization and matching of oil samples using fluorescence spectroscopy and parallel factor analysis. *Anal Chem* 77(7):2210–2217
- Balsley A, Hansen K, Fitzpatrick M (2014) Detection of oil within the water column. *Int Oil Spill Conf Proc* 2014(1):2206–2217
- Bidleman TE, Castleberry AA, Foreman WT, Zaranski MT, Wall DW (1990) Petroleum hydrocarbons in the surface water of two estuaries in the Southeastern United States. *Estuar Coast Shelf Sci* 30(1):91–109
- Bugden JBC, Yeung CW, Kepkay PE, Lee K (2008) Application of ultraviolet fluorometry and excitation-emission matrix spectroscopy (EEMS) to fingerprint oil and chemically dispersed oil in seawater. *Mar Pollut Bull* 56(4):677–685. doi:10.1016/j.marpolbul.2007.12.022
- Patra D, Mishra AM (2002) Total synchronous fluorescence scan spectra of petroleum products. *Anal Bioanal Chem* 373(4):304–309. doi:10.1007/s00216-002-1330-y
- Vandermeulen JH et al (1979) Sediment penetration of Amoco Cadiz oil, potential for future

- release, and toxicity. *Mar Pollut Bull* 10 (8):222–227. doi:10.1016/0025-326x(79)90294-7
7. Von Der Dick H, Kalkreuth W (1986) Synchronous excitation and three-dimensional fluorescence spectroscopy applied to organic geochemistry. *Org Geochem* 10 (1–3):633–639. doi:10.1016/0146-6380(86)90060-4
 8. Wakeham SG (1977) Synchronous fluorescence spectroscopy and its application to indigenous and petroleum-derived hydrocarbons in lacustrine sediments. *Environ Sci Tech* 11 (3):272–276. doi:10.1021/es60126a012
 9. Chen RF, Gardner GB (2004) High-resolution measurements of chromophoric dissolved organic matter in the Mississippi and Atchafalaya River plume regions. *Mar Chem* 89 (1–4):103–125
 10. Coble PG (2007) Marine optical biogeochemistry: the chemistry of ocean color. *Chem Rev* 107(2):402–418
 11. Coble PG, Green SA, Blough NV, Gagosian RB (1990) Characterization of dissolved organic matter in the Black Sea by fluorescence spectroscopy. *Nature* 348(6300):432–435
 12. Del Vecchio R, Blough NV (2004) On the origin of the optical properties of humic substances. *Environ Sci Tech* 38(14):3885–3891
 13. Guéguen C, Guo L, Yamamoto-Kawai M, Tanaka N (2007) Colored dissolved organic matter dynamics across the shelf-basin interface in the western Arctic Ocean. *J Geophys Res* 112 (C5):C05038. doi:10.1029/2006jc003584
 14. Helms JR et al (2008) Absorption spectral slopes and slope ratios as indicators of molecular weight, source, and photobleaching of chromophoric dissolved organic matter. *Limnol Oceanogr* 53(3):955–969
 15. Sierra MMD, Giovanela M, Parlanti E, Soriano-Sierra EJ (2006) 3D-fluorescence spectroscopic analysis of HPLC fractionated estuarine fulvic and humic acids. *J Brazil Chem Soc* 17:113–124
 16. Vodacek A, Blough NV, DeGrandpre MD, Peltzer ET, Nelson RK (1997) Seasonal variation of CDOM and DOC in the Middle Atlantic Bight: terrestrial inputs and photooxidation. *Limnol Oceanogr* 42(4):674–686
 17. Weishaar JL et al (2003) Evaluation of specific ultraviolet absorbance as an indicator of the chemical composition and reactivity of dissolved organic carbon. *Environ Sci Tech* 37 (20):4702–4708. doi:10.1021/es030360x
 18. Kowalczyk P et al (2009) Characterization of dissolved organic matter fluorescence in the South Atlantic Bight with use of PARAFAC model: interannual variability. *Mar Chem* 113 (3–4):182–196. doi:10.1016/j.marchem.2009.01.015
 19. Murphy KR, Stedmon CA, Waite TD, Ruiz GM (2008) Distinguishing between terrestrial and autochthonous organic matter sources in marine environments using fluorescence spectroscopy. *Mar Chem* 108(1–2):40–58. doi:10.1016/j.marchem.2007.10.003
 20. Stedmon CA, Bro R (2008) Characterizing dissolved organic matter fluorescence with parallel factor analysis: a tutorial. *Limnol Oceanogr* 6:572–579. doi:10.4319/lom.2008.6.572
 21. Stedmon CA, Markager S, Bro R (2003) Tracing dissolved organic matter in aquatic environments using a new approach to fluorescence spectroscopy. *Mar Chem* 82 (3–4):239–254. doi:10.1016/s0304-4203(03)00072-0
 22. Walker SA, Amon RMW, Stedmon C, Duan S, Louchouart P (2009) The use of PARAFAC modeling to trace terrestrial dissolved organic matter and fingerprint water masses in coastal Canadian Arctic surface waters. *J Geophys Res* 114:G00F06
 23. Alostaz M, Biggar K, Donahue R, Hall G (2008) Petroleum contamination characterization and quantification using fluorescence emission-excitation matrices (EEMs) and parallel factor analysis (PARAFAC). *J Environ Eng Sci* 7(3):183–197. doi:10.1139/s07-049
 24. Booksh KS, Muroski AR, Myrick ML (1996) Single-measurement excitation/emission matrix spectrofluorometer for determination of hydrocarbons in ocean water. 2. Calibration and quantitation of naphthalene and styrene. *Anal Chem* 68(20):3539–3544. doi:10.1021/ac9602534
 25. Ferreira AM, Micaelo C, Vale C (2003) Are coastal resources of NW Portugal fingerprinting hydrocarbons released from the Prestige accident? *Ciencias Marinas* 29(1):109–114
 26. González JJ et al (2006) Spatial and temporal distribution of dissolved/dispersed aromatic hydrocarbons in seawater in the area affected by the Prestige oil spill. *Mar Pollut Bull* 53 (5–7):250–259. doi:10.1016/j.marpolbul.2005.09.039
 27. Kim M et al (2010) Hebei Spirit oil spill monitored on site by fluorometric detection of residual oil in coastal waters off Taean, Korea. *Mar Pollut Bull* 60(3):383–389. doi:10.1016/j.marpolbul.2009.10.015
 28. Østgaard K, Jensen A (1983) Evaluation of direct fluorescence spectroscopy for monitoring aqueous petroleum solutions. *Int J Environ Anal Chem* 14(1):55–72

29. Santos-Echeandía J, Prego R, Cobelo-García A (2008) Influence of the heavy fuel spill from the Prestige tanker wreckage in the overlying seawater column levels of copper, nickel and vanadium (NE Atlantic ocean). *J Mar Syst* 72 (1–4):350–357. doi:10.1016/j.jmarsys.2006.12.005
30. Bianchi TS et al (2014) Deepwater horizon oil in Gulf of Mexico waters after 2 years: transformation into the dissolved organic matter pool. *Environ Sci Tech* 48(16):9288–9297
31. Conmy RN et al (2013) Submersible optical sensors exposed to chemically dispersed crude oil: wave tank simulations for improved oil spill monitoring. *Environ Sci Tech* 48 (3):1803–1810
32. Mendoza WG, Riemer DD, Zika RG (2013) Application of fluorescence and PARAFAC to assess vertical distribution of subsurface hydrocarbons and dispersant during the Deepwater Horizon oil spill. *Environ Sci* 15 (5):1017–1030
33. Zhou Z, Guo L (2012) Evolution of the optical properties of seawater influenced by the Deepwater Horizon oil spill in the Gulf of Mexico. *Environ Res Lett* 7(2):025301. doi:10.1088/1748-9326/7/2/025301
34. Zhou Z et al (2013) Characterization of oil components from the Deepwater Horizon oil spill in the Gulf of Mexico using fluorescence EEM techniques. *Mar Chem* 148:10–21. doi:10.1016/j.marchem.2012.10.003
35. Zhou Z, Liu Z, Guo L (2013) Chemical evolution of Macondo crude oil during laboratory degradation as characterized by fluorescence EEMs and hydrocarbon composition. *Mar Pollut Bull* 66(1–2):164–175
36. Douglas GS, Owens EH, Hardenstine J, Prince RC (2002) The OSSA II pipeline oil spill: the character and weathering of the spilled oil. *Spill Sci Technol Bull* 7(3):135–148. doi:10.1016/S1353-2561(02)00046-4
37. Beltrán JL, Ferrer R, Guiteras J (1998) Multivariate calibration of polycyclic aromatic hydrocarbon mixtures from excitation-emission fluorescence spectra. *Anal Chim Acta* 373 (2–3):311–319
38. Blough NV, Del Vecchio R (2002) Chromophoric DOM in the coastal environment. In: Hansell DA, Carlson CA (eds) *Biogeochemistry of marine dissolved organic matter*. Academic, San Diego, pp 509–546
39. Coble PG (1996) Characterization of marine and terrestrial DOM in seawater using excitation-emission matrix spectroscopy. *Mar Chem* 51(4):325–346. doi:10.1016/0304-4203(95)00062-3
40. Coble PG, Del Castillo CE, Avril B (1998) Distribution and optical properties of CDOM in the Arabian Sea during the 1995 Southwest Monsoon. *Deep Sea Res II Top Stud Oceanogr* 45(10–11):2195–2223. doi:10.1016/S0967-0645(98)00068-x
41. Guéguen C, Guo L, Tanaka N (2005) Distributions and characteristics of colored dissolved organic matter in the Western Arctic Ocean. *Cont Shelf Res* 25(10):1195–1207
42. Stedmon CA, Markager S, Kaas H (2000) Optical properties and signatures of chromophoric dissolved organic matter (CDOM) in Danish coastal waters. *Estuar Coast Shelf Sci* 51(2):267–278
43. Twardowski MS, Boss E, Sullivan JM, Donaghay PL (2004) Modeling the spectral shape of absorption by chromophoric dissolved organic matter. *Mar Chem* 89(1–4):69–88
44. Ohno T (2002) Fluorescence inner-filtering correction for determining the humification index of dissolved organic matter. *Environ Sci Tech* 36(4):742–746
45. Ferretto N et al (2014) Identification and quantification of known polycyclic aromatic hydrocarbons and pesticides in complex mixtures using fluorescence excitation - emission matrices and parallel factor analysis. *Chemosphere* 107:344–353
46. Lorenzo-Seva U, ten Berge JMF (2006) Tucker's congruence coefficient as a meaningful index of factor similarity. *Methodology* 2(2):57–64
47. Cecil TL, Rutan SC (1990) Correction for fluorescence response shifts in polycyclic aromatic hydrocarbon mixtures with an innovations-based Kalman filter method. *Anal Chem* 62 (18):1998–2004
48. Tucker SA, Acree WE, Cho BP, Harvey RG, Fetzer JC (1991) Spectroscopic properties of polycyclic aromatic hydrocarbons: effect of solvent polarity on the fluorescence emission behavior of select fluoranthene, fluoreno-chrysene, indenochrysene, and indenopyrene derivatives. *Appl Spectrosc* 45 (10):1699–1705
49. Murphy KR, Stedmon CA, Graeber D, Bro R (2013) Fluorescence spectroscopy and multi-way techniques. *PARAFAC Anal Methods* 5 (23):6557–6566. doi:10.1039/c3ay41160e
50. Andersen CM, Bro R (2003) Practical aspects of PARAFAC modeling of fluorescence excitation-emission data. *J Chemometr* 17 (4):200–215. doi:10.1002/cem.790